Lab on a Chip

Accepted Manuscript

This is an *Accepted Manuscript*, which has been through the Royal Society of Chemistry peer review process and has been accepted for publication.

Accepted Manuscripts are published online shortly after acceptance, before technical editing, formatting and proof reading. Using this free service, authors can make their results available to the community, in citable form, before we publish the edited article. We will replace this *Accepted Manuscript* with the edited and formatted *Advance Article* as soon as it is available.

You can find more information about *Accepted Manuscripts* in the **Information for Authors**.

Lab Chip

Dynamic Article Links ▶

Technical Innovation

Low cost lab-on-a- chip prototyping with a consumer grade 3D printer

Germán Comina,[a] Anke Suska[a] and Daniel Filippini*[a]

Versatile prototyping of 3D printed lab-on-a-chip devices, supporting different forms of sample delivery, transport, functionalization and readout, is demonstrated with a consumer grade printer, which centralizes all critical
10 **fabrication tasks. Devices cost 0.57US$ and are demonstrated in chemical sensing and micromixing examples, which exploit established principles from reference technologies.**

Classical microfabrication techniques support the complete range of lab-on-a-chip (LOC) configurations and functions;[1,2,3]
15 however, they involve specialized resources and skills beyond the scope of many potential LOC users.[4] Simplified processes have been explored, leading to the elimination of photolithographic masks[4,5,6] and even to the use of routine microscopes as microfabrication platforms.[7] Still these approaches require
20 dedicated skills and clean room services, for complementary processes.

Direct fabrication of 3D structures can be subtractive, such as in laser writing[8] and computer numerical control milling[9], or additive like in thermoplastic extrusion systems[10] and micro
25 stereo lithography platforms[6]. Relative advantages of these and other existing 3D structuring technologies have been reviewed[11] and refer to type and variety of materials they can employ as well as the platform cost, achievable resolutions, surface roughness, complexity, cost of materials and maintenance.
30 LOC microfabrication with 3D printers was initially demonstrated with custom-made systems[12], and later extended to more affordable additive printing systems[13] able to combine different materials for reactionware and millifluidics[14]. Recently, we demonstrated micro fabrication of templates for classical
35 PDMS on glass LOC (PDMS-LOC) using consumer grade 3D micro stereo lithography (MS) printers (2290 US$, Miicraft[15]). The technique is compatible with usual LOC dimensions and delivers sub-micrometric surface roughness;[16] however, further exploration of 3D printing possibilities could entirely eliminate
40 templates and transfer all fabrication specialized tasks to the printer, thus completely disengaging design complexity from fabrication skills. The implications entail custom LOC access with minimum infrastructure and highly versatile microfabrication compatible with flexible prototyping and
45 immediate exploitation.

The value of a prospective fabrication platform can be gauged by its ability to accommodate different designs and principles using essentially the same tool. This work demonstrates fabrication of LOC devices, designed around a 3D printed single
50 monolithic body, or unibody LOC (ULOC), which can be easily completed with simple complementary materials and procedures.

The versatility of ULOC is demonstrated through the integration of printed connectors, complex geometric features to facilitate functionalization, the incorporation of lateral flow
55 transport[17] capabilities, and the inclusion of glass micro beads in continuous flow mixers.

This first demonstration of ULOC illustrates passive and active transport as well as other accessory functions that can be directly migrated from PDMS-LOC, lateral flow[17,18] and micro beads[19]
60 supported systems. The devices are compatible with fluorescence microscopy and color imaging readout, and were applied to H_2O_2 and glucose detection.

Devices in this work cost in average 0.57 US$/device, and can be fabricated within 30min, thus offering an affordable and agile
65 breadboard for LOC optimization.

ULOC devices described in this work are possible due to the resolution presently achievable with consumer grade MS 3D printers. Previous demonstrations of 3D printed fluidics, made
70 with affordable thermoplastic extrusion systems[14], imposed restrictions on resolution and surface roughness, which prevented regular LOC channel geometries and simple sealing procedures.

In contrast, last generation of affordable MS 3D printers,[13,15,16]
75 aided by digital micro mirror devices (DMD), deliver resolutions in the 50µm range, and surface roughness under 182nm (see ESI), which enables efficient sealing with regular adhesive tape or PDMS films. For similar resolutions other advanced additive systems are about 10 to 100 times[20] more expensive that the
80 Miircraft printer used in this work. On the other hand, those systems are capable of combining different materials and can print larger objects.

The printer software transforms computer-aided designs (CADs) into bitmap image collections (black and white .png
85 format), corresponding to cross-sections of the 3D design, spaced at 50µm steps in the vertical direction. Each of these images is sequentially displayed in the DMD element to cure each layer of the 3D printout. These bitmap images can be edited and provide an easy way to modify the design with common image retouching
90 software, such as Microsoft Paint® or Photoshop®, instead of

editing the CAD source, which is a more specialized alternative.

Fig. 1a illustrates a design integrating connectors, roofed micro channels and 100μm thin suspended structures in the same body. The connectors were designed for direct plugging of 1mm inner
5 diameter silicone tubing, used for standard connection with auxiliary fluidic and sample delivery systems.

10
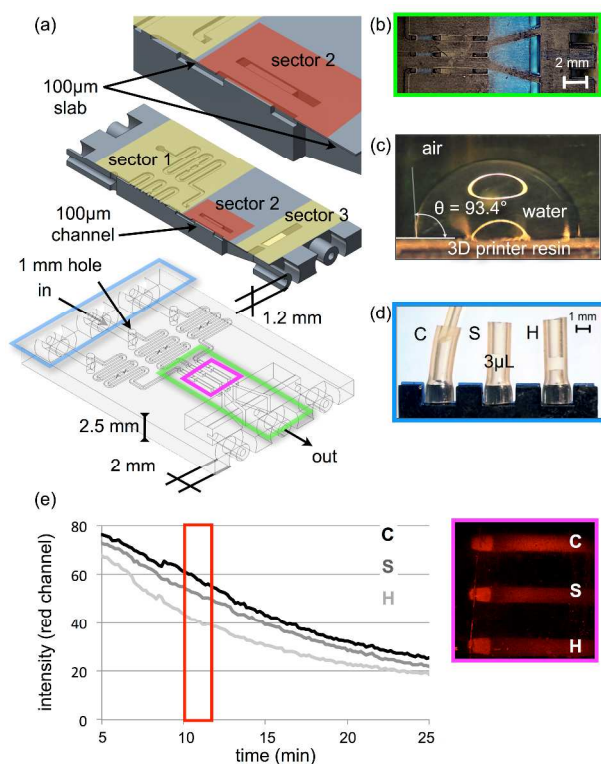
Fig. 1a) ULOC design showing details of silicone tubing connectors and
15 geometric features for independent sealing of different sectors. Channels are 500μm wide and 200μm deep, except for the sector 2, where they are 100μm deep. b) Picture of the unibody before sealing.c) Water drop on printed resin showing a contact angle of 93.4°. d) Detail of the 3D printed connector with 3μl samples of H_2O_2 solutions pipetted
20 into the silicone tubing. Teflon tubing connected to a 5ml syringe is used to manually pump the samples to the measuring region. e) The inset shows the fluorescence image of the detection region for three H_2O_2 concentrations, control (C), sample (S) and high level (H). Regions of interest from these channels were used to extract the time response,
25 which was acquired at 10s intervals. Red square indicates the interval used for sensitivity quantification.

Unibody connectors (Fig. 1a) lead to the microchannels via through holes, which contribute to the efficient removal of
30 unexposed resin, and can be exploited for fluidics purposes, as shown later. Three 500μm wide and 200μm deep channels, with 50μm wide hindrances, were accommodated in the same device, to integrate the calibration range of the H_2O_2 detection example.

In order to simplify the fabrication procedure, the unibody is
35 conceived to accept separately prepared functional surfaces.

Accordingly, different channel sectors must be able to seal independently, which in this case was solved with a 100μm thick roofed channel (detail Fig. 1a) bridging the space between sector1 and sector2. Sector2 was sealed with a PDMS film separately
40 functionalized for H_2O_2 fluorescent detection,[21] and the long part of the micro channels, under sector1, introduces a time delay that permits controlled delivery of fixed sample volumes, when the device is used for manual delivery. Sealing of regions 1, 3 and the backside, were completed with adhesive tape (3M Ruban
45 Adhesive Scotch∖ Nastro Adhesive).

Defining features of a 3D design, such as channels, can be made along the z-axis, or on the xy-plane with the z-axis displacement configuring the thickness of the planar design. The first alternative is the natural mode of additive 3D printing, and in
50 the case of thermoplastic extrusion systems there is not much difference in the final result. The situation drastically changes with MS 3D printers, where an entire low roughness xy-plane is exposed every 7s. To exploit this characteristic, unibodies are made planar, resulting in minimal roughness that allow
55 complementary tape sealing. As a consequence long channels can be created open, not sacrificing reliability and with minimal texture. This use of the printing direction also permits to exploit the resolution limits, since 50μm deep channels are easier to clean from uncured resin than 500μm deep elements.

60 The same printer used in the conventional fabrication direction[24] takes several hours to produce similar size prototypes, restricts the minimum channel cross section compatible with resin release to 1000μm×500μm, and leaves the quality surface finishing unexploited.

65 In ULOC, unexposed resin is removed by 20s sonication in industrial grade ethanol after which the unibody is air-dried and ready for assembly. Uncured resin can be problematic to evacuate from confined spaces, such as long roofed channels, and the 2mm long section separating sector1 and sector2 was a conservative
70 compromise between the required functionality and fabrication reliability.

The blue resin composition is proprietary information, and the material safety data sheet only reports that is a modified acrylate oligomer and monomer in combination with an epoxy monomer,
75 a photo initiator, and additives[15].

UV-curable formulations use oligomers or prepolymers consisting of reactive sites based on functional acrylate groups to limit volatile emissions, whereas the use of epoxy enables versatile tailoring of properties such as viscosity, harness and
80 chemical compatibility[22,11].

The surfaces of numerous commodity polymeric materials that are suitable with microfabrication are not inert and interfere with chemical detection or cell viability, thus requiring specific surface conditioning[23]. In this work chemical functionalization is
85 carried out in well-described substrates such as PDMS in the case of H_2O_2 detection and cellulose powder for glucose measurements. The ULOC assembly allows migrating these established solutions to the unibody. Printed structures are hydrophobic (93.4° contact angle in Fig. 1c), which complement
90 well with the confinement of aqueous solutions and for the cellulose passive transport configuration (Fig. 2).

The use of printed templates for the fabrication of PDMS LOC[16] showed that templates can be exposed to 65°C for several

hours and still be reused, suggesting sufficient thermal stability, although for the purpose of this work the entire fabrication and characterization was made at room temperature.

5 A newer clear type of resin, which is reported with the same composition as the blue resin[15], has been shown compatible with droplet extraction using a decanol organic phase, and with electrophoretic separation[24]. Custom formulations of epoxy acrylates are known to be compatible with LOC uses[11,23], and eventually tailoring the resin chemistry could expand the range of 10 compatible uses, meanwhile the unibody offers a breadboard where to integrate proven materials and solutions within a communal assembly.

PDMS was functionalized for H_2O_2 detection (Fig. 1e)[25,26]. H_2O_2 concentration in blood and urine has been suggested as a 15 biomarker for oxidative stress in humans,[27] which is associated with the development of numerous serious conditions such as cancer[28] and heart failure[29].

For H_2O_2 detection with ULOC, connectors were assembled with silicon tubing (Fig. 1d), and 3µl of control solution (C), 20 0.1µM (S) and 1µM (H) H_2O_2 in saline solution were pipetted into the tubing, and later pumped into the device using an air loaded 5mL syringe. These concentrations test the lowest clinically relevant limit of H_2O_2 in urine for oxidative stress monitoring.[27]

25 The device was designed for fluorescence microscope readout and the inset shows the three separately sealed channels in the detection zone (insert in Fig. 1e), Time-lapse acquisition, at 10s intervals, captured the assay time response from which a sensitivity of 15.22 intensity units/µM, with a resolution of 30 0.098µM, evaluated within the [10,12] min interval could be estimated.

Protocols for H_2O_2 detection in aqueous solution[25,26,30] were adapted to ULOC from established configurations (see ESI). In this assay, horseradish peroxidase (HRP) catalyzed the de-N-35 acetylation and oxidation of non-fluorescent Ampliflu-Red by H_2O_2 to highly fluorescent resorufin[21]. Resorufin is also a substrate for HRP, which leads to the total consumption of the fluorescent product after a while (Fig. 1e). Time response features depend on the initial concentration of H_2O_2, and can be 40 adapted to the desired detection range with the assay proportions, as has been shown elsewhere[16].

To demonstrate the versatility of ULOC to accommodate different configurations, a lateral flow device was implemented around the unibody concept, for the detection of glucose. 45 Monitoring of glucose in blood (glycemia) is central for control of diabetes mellitus, which affects 2% of the world population and 6% of adult population in the western world, and is the most representative biosensing target involving 85% of the biosensing market.[31,32]

50 The ability to modify a core design, without extensive knowledge of CAD operation, is a bonus for biosensor developers whose focus is beyond microfabrication. With the 3D printer the exposure patterns are bitmap images that can be edited with image retouching software. In the present case, the first device 55 (Fig.1) was transformed into the lateral flow example (Fig. 2) using only Photoshop® edition. The possibility to image edit exposure patterns can significantly shorten the workflow during the development phase, since it avoids CAD re-edition, slicing

and control procedures, by just correcting the few bitmaps that 60 define the design.

Fig. 2a shows the fabricated device with channels filled with cellulose powder paste, which were locally functionalized for glucose detection. The image corresponds to the final response after the sensing surface has been exposed to a control (C) and 65 two glucose concentrations (H and S) within the diagnostic range.[33]

Cellulose powder is a well-established material for thin layer chromatography[34] and provides passive capillary transport[35] in this lateral flow configuration. The hydrophobic channels in the 70 printed unibody, naturally confine the flow within the cellulose powder, which can be easily delivered into the channels by simple procedures (see ESI).
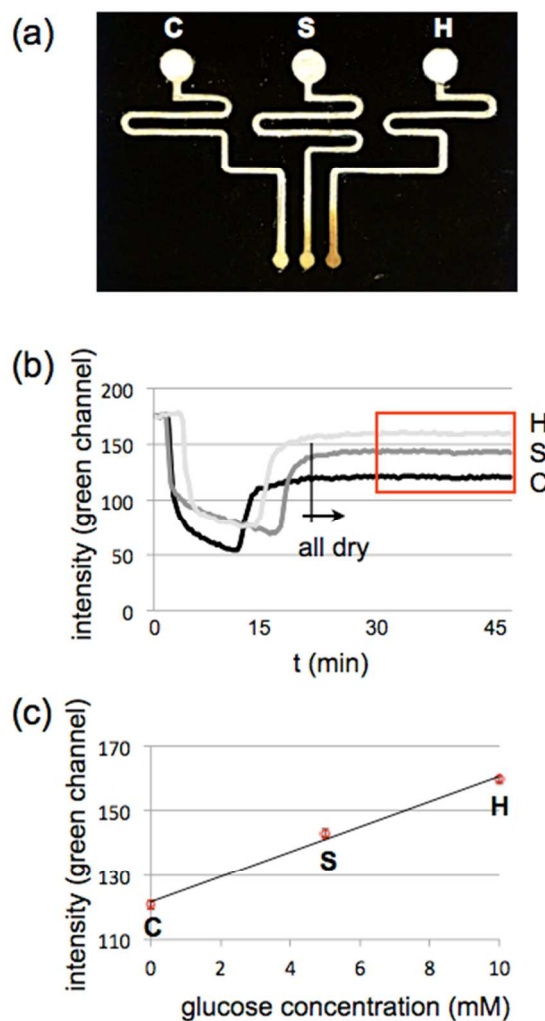
Fig. 2a) Picture of the printed device converted into a lateral flow device 75 by the inclusion of cellulose powder tracks functionalized for glucose detection. b) Time response of the glucose test for control sample (C), 5mM (S) and 10mM (H) of glucose. The steady response of the dry assay is highlighted with a red frame. c) Quantification of the glucose concentration from the steady response in b).

80 Time-lapse acquisition of the glucose test response, imaged at 20s intervals with a Galaxy Note2 8Mpix rear side camera, renders a low noise response (Fig. 2b). Light absorption in the green camera channel increases when the detection area gets wet

with the sample, and once dried, a 10min interval was allowed for response stabilization, after which the average response in the last 15min was used for quantification, rendering the observed linear behavior (Fig. 2c). From these measurements a sensitivity of 3.9 intensity units/mM with a resolution of 0.56mM (or 0.50 mg/dL) could be estimated.

The assay uses a colorimetric detection principle (see ESI). In the presence of glucose and oxygen, glucose oxidase (GOx) catalyzes the oxidation of glucose to glucono delta-lactone and hydrogen peroxide, which is used by HRP to catalyze the oxidation of colorless iodide to brown iodine[36] monitored in the measurement.

The final LOC functionality tested here in ULOC configuration is the integration of micromixers. Mixing is a common preparatory stage in chemical analyses, and accordingly, an important function for LOCs that must be supported by any prospective fabrication method. Microfluidic dimensions favor laminar flow regimes, where mixing occurs as a slow diffusional process, and different designs exist to favor turbulence and better mixing performance.[37] Chaotic mixers[12,37,38] are one possibility to improve performance, and have been demonstrated on PDMS-LOC created on 3D printed templates.[16]
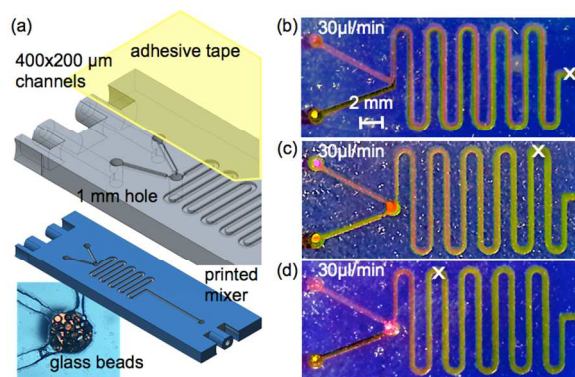
Fig. 3a) Mixer design with through hole used for fluidic purposes. The channels are 400µm wide and 200µm deep. b) Diffusion mixer image with 1mM fluorescein and 1mM rhodamine B flowed at 30µl/min. c) Mixer with through hole, measured at the same flow rate as b). d) Mixer with through hole filled with micro beads, and measured in the same conditions as b). White crosses highlight the position where the streams mix.

Here a different approach is investigated. The Reynolds number in a channel is proportional to the channel height[38], and thus a simple geometric feature, such as a 1mm through hole, at the join between flows can improve the mixing efficiency in a very compact way. Additionally, the through hole allows to incorporate glass micro beads to favor turbulent regimes, and simultaneously the ULOC design helps to introduced the beads from the device backside, thus avoiding problematic bead spillover that can compromise the front side sealing. In this case, the device was first sealed from the front side and then loaded with beads from the backside, and finally taped from the backside.

To assess the mixing performance, the devices were flowed with fluorescein and rhodamine B aqueous solutions, delivered with two syringe pumps at 30µl/min.

A diffusional mixer (Fig. 3b), without the through hole, was used to compare performances, and shows 2 unmixed streams at the distal end of the device (highlighted by a white cross). When the through hole feature was added (Fig. 3c), the mixing behavior changed and the flow divided in three apparent streams, almost entirely mixing (single color) at the end of the device (~80% of the channels length), whereas with the beads (Fig. 3d), only one color stream could be distinguished at ~40% of the channel length, thus providing a compact possibility to double the mixing efficiency.

Results in this work demonstrate the possibility of 3D printed LOC devices compatible with different sample delivery, transport and detection approaches. In all cases, migration from established solutions, in classical LOC, was shown possible and simple, whereas ULOC fabrication demands minimal efforts and infrastructure.

The roofed channel used to separate independent sealed sectors (Fig. 1) also illustrates the advantage of direct additive printing respect to replicas from templates. Independently of the technology used to create the template, a seemly trivial roofed element cannot be produced in a single manufacturing step. On the other hand, templates are reusable, whereas direct printing implies reprinting each new device. Unibody optimizes additive prototyping by minimizing the device thickness and by exploiting the planar dimension, where the printer can deliver sub micrometric surface roughness and reliable resin removal in small features over long distance ranges.

Conclusions

In this work, affordable 3D printed LOC devices have been demonstrated. Complex geometries, directly created in 3D printed structures, enable transference of demanding fabrication tasks to the printer, thus maximizing reliability and removing the influence of user fabrication skills from the prototypes.

These capabilities have been investigated with devices serving H_2O_2 and glucose detection, using passive and active transport, as well as configurations suitable with fluorescence and colorimetric readout. In addition with continuous flow micro mixers, these results demonstrate a versatile set of essential configurations for LOC systems.

Consumer grade MS 3D printers not only simplify access to custom LOC designs, but can also accommodate sophisticated features only accessible in advanced LOC fabrication techniques. These aspects were shown possible, at a convenient development cost of 0.57US$/device, and for prototype fabrication times under 30 min.

3D printed ULOC devices offer a breadboard for experimentation that is compatible with fast and affordable prototype optimization, which can exploit established LOC solutions.

Acknowledgments

Lab on a Chip Accepted Manuscript

Science Technologies (LIST), Sweden.

Notes and references

*ᵃ Optical Devices Laboratory – Department of Physics, Chemistry and Biology (IFM), Linköping University, Linköping 58183, Sweden. *E-mail:*
5 *danfi@ifm.liu.se; Tel: +46 13 281282.*

1   S. Mitra, S. Chakraborty Editors, in *Microfluidics and Nanofluidics Handbook*, Fabrication, Implementation, and Applications, CRC Press Taylor & Francis Group, Boca Raton 2012.
2   A. Foudeh, T. Didar, T. Veresa, M. Tabrizian, *Lab Chip*, 2012, **12**, 3249.
3   I. Dimov, L. Basabe-Desmonts, J. Garcia-Cordero, B. Ross, A. Ricco, L. Lee, *Lab Chip*, 2011, **11**, 845.
4   J. Love, D. Wolfe, H. Jacobs, G. Whitesides, *Langmuir*, 2001, **17**, 6005.
5   J. Behm, K. Lykke, M. Pellin, J. Hemminger, *Langmuir*, 1996, **12**, 2121.
6   C. Sun, N. Fang, D. Wu and X. Zhang, *Sens. Actuators, A*, 2005, **121**, 113.
7   P. Preechaburana, D. Filippini, *Lab Chip*, 2011, **11**, 288.
8   Y. Liao, et al., *Lab Chip*, 2013, **13**, 1626.
9   M. Camara, J. Campos Rubio, A. Abrao, J. Davim, *J. Mater. Sci. Technol.*, 2012, **28**, 673.
10 J. McDonald, M. Chabinyc, S. Metallo, J. Anderson, A. Stroock, G. Whitesides, Anal. Chem., 2002, **74**, 1537.
11 A. Waldbaur, H. Rapp, K. Lange, B. Rapp, *Anal. Methods*, 2011, **3**, 2681
12 D. Therriault, S. White, J. Lewis, *Nature Materials*, 2003, **2**, 265.
13 B. Evans, in Practical 3D Printers: The Science and Art of 3D Printing, APress, c/o Springer Science+Business Media, LLC,233 Spring Street, New York, NY 10013, USA, 2012.
14 M. Symes, P. Kitson, J. Yan, C. Richmond, G. Cooper, R. Bowman, T. Vilbrandt, L. Cronin, *Nature Chemistry*, 2004, **4**, 349.; P. Kitson, M. Rosnes, V. Sans, V. Dragone, L. Cronin, *Lab Chip*, 2012, **12**, 3267.
15 MiiCraft®, MiiCraft 3D Printer, http://www.miicraft.com/products/ (accessed August, 2013)
16 G. Comina, A. Suska, D. Filippini, *Lab Chip*, 2014, **14**, 424.
17 R. Wong, l. Harley, Y. Tse Editors in Lateral Flow Immunoassay, Humana Press, c/o Springer Science+Business Media, LLC, 233 Spring Street, New York, NY 10013, USA,
18 C. D. Chin, V. Linder and S. K. Sia, *Lab Chip*, 2012, **12**, 2118.
19 N. Lee, Y. Yang, Y. Kim, S. Park, *Bull. Korean Chem. Soc.*, 2006, **27**, 479.
20 http://envisiontec.com/products/micro/; http://www.stratasys.com/3d-printers/design-series/precision/objet-connex500
21 Zhou, M.; Diwu, Z.; Panchuk-Voloshina, N.; Haugland, *Anal. Biochem*, 1997, **253**, 162; and details in ESI.
22 D. Chattopadhyay, S. Panda, K. Raju, *Progress in Organic Coatings*, 2005, **54**, 10.
23 J. Liu, X. Sun, M. Lee, *Anal. Chem.*, 2005, **77**, 6280.
24 A. Shallan, P. Smejkal, M. Corban, R. Guijt, M. Breadmore, *Anal. Chem.*, 2014, **86**, 3124.
25 V. Towne, M. Will, B. Oswald, Q. Zhao, *Analytical Biochemistry*, 2004, **334**, 290.
26 I. Julca, M. Alaminos, J. González-López, M. Manzanera, *Biotechnol Adv*, 2012, **30**,1641.
27 J. Yuen, I. Benzie, *Free Radic Res*, 2003, **37**, 1209.
28 B. Halliwell, *Biochem. J*, 2007, **401**, 1.
29 N. Singh, A.K. Dhalla, C. Seneviratne, P.K. Singal, *Molecular and Cellular Biochemistry*, 1995, **147**, 77.
30 D. Bodas, C. Khan-Malek, *Sens. Actuators B*, 2007, **123**, 368.
31 J. Newman, A. Turner, *Biosens. Bioelectron.*, 2005, **20**, 2435.
32 Turner, APF., Gifford, R., 2013. Implanted Sensors in Filippini, D., (Ed.) Autonomous Sensor Networks: Collective sensing strategies for analytical purposes, 159-190. Springer Series on Chemical Sensors and Biosensors 13.
33 S.F. Clarke, J.R. Foster, *Br J Biomed Sci*, 2012, **69**, 83.
34 B. Fried, J. Sherma in *Thin-layer chromatography*, Marcel Dekker, New York, 1999.
35 M. Zimmermann, H. Schmid, P. Hunziker, E. Delamarche, *Lab Chip*, 2007, **7**, 119.
36 J. Peele, R. Gadsden, R. Crews, *Clin. Chem*, 1977, **23**, 2242.
37 Y. Suh, S. Kang, *Micromachines*, 2010, **1**, 82.
38 N. Nguyen, Z. Wu, *J. Micromech. Microeng*, 2005, **15**, R1.

Lab on a Chip Accepted Manuscript